Electrical Power and Energy Systems 131 (2021) 107083

Contents lists available at ScienceDirect

International Journal of Electrical Power and Energy Systems

journal homepage: www.elsevier.com/locate/ijepes

Enhanced partial frequency variation starting of hydroelectric pumping units: Model based design and experimental validation

Andrea Vicenzutti *, Massimiliano Chiandone, Vittorio Arcidiacono, Giorgio Sulligoi

Dept. of Engineering and Architecture, University of Trieste, Trieste, Italy

ARTICLE INFO

Keywords:
Hydroelectric power plant
Pumped Storage
Synchronous motor starting
Excitation Control System
Model-based design
Experimental validation

ABSTRACT

The hydroelectric pumped storage is one of the most sustainable solutions to store electrical energy for optimizing the grid operation. However, the pump motor starting may constitute a significant issue for the power plant. Indeed, the motor's large power and the long power lines (needed for connecting remotely located plants to the grid) may prevent a direct-on-line start. On the other hand, constraints as spaces availability in the powerhouse, and time and cost availability (especially for revamping projects) limit the feasibility of other starting methods. In this paper, a novel starting method is proposed for the revamping of a hydroelectric power plant (HPP), where a synchronous machine is used to drive the pump. On the basis of the power plant characteristics, an enhanced version of the synchronous starting with partial frequency variation is proposed, leading to the creation of a startup sequence capable of being integrated into the existing excitation control systems' software (of both the generator and the motor installed in the power plant). Such Enhanced Partial Frequency Variation (EPFV) starting method combines the advantages of back-to-back starting method to the ones of asynchronous starting, without requiring additional equipment in respect to a conventional direct-on-line start solution. This is enabled by the model-based design approach here applied, which allows to determine the correct set of parameters and variables' thresholds required for the machine startup, taking into account the specific characteristics of the HPP in study. The developed starting sequence, implemented into the real HPP by using the capabilities of the existing digital excitation control systems, allowed the correct starting of the motor. This is demonstrated by experimental data obtained during the 5MVA motor starting tests. The results also prove the effectiveness of the model-based design approach in enabling the definition of the pump starting sequence, as well as validating the mathematical model used for the sequence design.

1. Introduction

The renewable sources quota in electrical energy production is steadily increasing. However, most of these power sources are distributed ones, which are frequently characterized by a poor programmability (e.g. photovoltaic systems). Moreover, at present renewable sources have a priority in dispatching, which makes them operating similarly to base load power plants. These facts have prevented most of them from delivering full support to the transmission system's voltage and frequency regulation. As an example, thermal power plants based on biofuels and hydroelectric power plants (HPPs) are fully integrated into the conventional voltage and frequency regulation architecture. Conversely, at present photovoltaic and wind generators limit their intervention to the disconnection from the grid upon reaching given voltage or frequency limits. Such a behavior may cause unwanted variations in grid power and potentially leads to grid control degradation, since renewable power sources are replacing a significant quota of traditional regulating power plants. Thus, in the last years much attention is given to energy storage technologies [1–4] suitable for providing grid regulation and peak shaving services.

Despite the technical advancements in chemistry-based energy storage systems, at present hydroelectric pumped storage plants constitute most of the electrical system's storage capacity. Such a technical solution is based on the exploitation of water's potential energy, which is pumped in a higher altitude basin during the periods with high production from renewables and low demand. Given the fast response of water turbines, when grid's power demand rises such turbines can be used to generate power useful for grid's peak shaving.

* Corresponding author.
E-mail addresses: avicenzutti@units.it (A. Vicenzutti), mchiandone@units.it (M. Chiandone), vittorio.arcidiacono@libero.it (V. Arcidiacono), gsulligoi@units.it (G. Sulligoi).

https://doi.org/10.1016/j.ijepes.2021.107083
Received 13 November 2020; Received in revised form 27 January 2021; Accepted 2 April 2021
Available online 30 April 2021

Therefore, the pumped storage systems are considered one of the best means for storing high amounts of electrical energy for optimizing the overall power grid operation [5–10], thanks to their high efficiency, high power, and significant energy level. In this regard, the installation (or revamping) of hydroelectric pumped storage plants represents an approach able to ensure the correct power grid operation with actual and future renewables penetration [11], as well as increasing its sustainability. However, the most significant issue in exploiting pumped storage systems is the need of a usable basin and specific conditions regarding water availability throughout the year. Moreover, other technical and non-technical aspects can deeply affect the decision of building such systems. Indeed, at present most locations where a pumped storage system installation is affordable have already been used in many countries, thus limiting the improvement in the total storage capacity achievable by means of new installations. To overcome such an issue, some peculiar proposals have been made, such as the underground pumped hydro storage [12]. Though, the pumping function introduction into existing HPP may be another possible approach, as well as the exploitation of basins built for other aims (e.g., water reservoirs, agricultural irrigation). Such approach is being currently applied because, besides the achievable advantages for system operators, the pumped storage is a new business opportunity for hydroelectric plants' owners. In fact, the latter are aiming at selling energy storage services to system operators, for compensating non-dispatchable energy sources.

When considering pumped storage systems, one of the most frequent problems is related to the pump's motor starting. In fact, a careful evaluation of available starting methods is needed in order to successfully start a large power motor at the end of a long power line (needed since such power plants are commonly placed in remote areas) [13]. While most of the recent literature is focused on synchronous permanent magnet or reluctance motors starting and control [14,15], conventional synchronous machines are still the most used ones in industrial systems [16]. Regarding the latter type of synchronous motors, their starting has been studied in depth, both in the past [17–20] and in recent times [21–26]. Moreover, concerning the specific issue of pumping units in HPPs, some analyses can be found in [27,28]. In this regard, the exploitation of up-to-date technologies can be useful to allow for a less impacting introduction of the pumping function in an HPP, or to improve the starting performance of an existing pump.

In this paper, a novel technical solution for starting a synchronous motor pump in a pumped storage system is described. In particular, an enhanced partial frequency variation (EPFV) starting sequence is proposed, capable of coupling the advantages of both back-to-back starting (e.g., limited currents during startup) with the ones of asynchronous starting (e.g., reduced number of required components, and high starting torque). Such a technical solution can be used to enable the pump motor start in HPPs located in remote areas and/or characterized by limited space availability, thus allowing to integrate the pumping function in existing HPPS by only installing the pump. In fact, the solution described and tested in this paper allows assuring the pump's correct starting without generating transients on the power grid, at the same time using the same components that are required for the simple direct-on-line start solution. The starting sequence here proposed is implemented in a real system by means of two digital Excitation Control Systems (ECSs) [29], after having defined its main parameters and demonstrated its effectiveness by means of a model-based design approach. Moreover, the proposed starting sequence enables the coordinated action of the two machines (generator and motor) to achieve the pump starting, the power grid synchronization, and the subsequent generator stop by the independent action of the two ECSs. Thus, no dedicated coordination control system or communication link among the two machines' ECSs are required, no additional equipment has to be installed (which is a critical point of modern converter-based starting approaches), no surveillance or manual action by experienced operators is needed, and the cost of the starting system is very low.

The paper is organized as follows: A brief description of the HPP is presented in Section 2, while Section 3 describe all the motor starting methods applicable to the machine available in the HPP in study, motivating the specific choice here made. Section 4 depicts the starting sequence which has been conceived, in order to provide the successful start of the motor despite the peculiarities of the specific application. In Section 5, the modeling and simulation activities performed to correctly define the starting sequence steps, its required variables, and its thresholds, are described. Section 6 presents the implementation of the EPFV in the real system. In particular, it describes the digital ECS control platform and the starting sequence implementation, presents and discusses the experimental data from the commissioning tests, and provides a validation of the simulation results by comparing them with the experimental results. Finally, conclusions are given in Section 7.

Table 1
HPP machines data.

Machine	Hydraulic Turbine		Pump	
Type	Double jet Pelton		Four stage, with pre-pump	
Head [m]	302–313		340	
Flow [m^3/s]	1.6		1	
Speed [rpm]	600		1000 (main pump)	
Mechanical Power [MW]	4.32–4.4		3.875 (included 200 kW for the pre-pump)	
Electrical Power [MVA]	5		4.7 (pre-pump included)	
Voltage [kV]	11.5		11.5	
Power factor	0.9		0.9	
Rated current [A]	251		242	
Field current no load [A dc]	135		140	
Reactances (%) and time	Xd	Xq 109.1	Xd	Xq 111.5
constants (s)	110.4	X'q	112.5	X'q
Non saturated data	X'd 23.1	109.1	X'd 19.9	111.5
	X"d	X"q 5.6	X"d	X"q 17.1
	16.7	T'do	13.7	T'do
	T'd 0.36	1.74	T'd 0.35	1.96
	T"d	T"do	T"d	T"do
	0.03	0.04	0.04	0.06
	T"q	T"qo	T"q	T"qo
	0.03	0.16	0.05	0.35
	Ta 0.11		Ta 0.09	

2. Hydroelectric power plant description

This paper addresses the definition, implementation, and commissioning of the starting procedure for the pumping section of a revamped pumped storage HPP located in the Northern Italy Alps. The HPP exploits a catchment basin with a capacity up to 8.3 million m^3 and a 340 m gross head. The original plant was designed with pumped storage function already embedded. Such plant was sized to maximize its production over the year, by taking into account for the different yearly water availability in the lower and upper basins. To this aim, two reversible three phase asynchronous machines were installed, connected to two hydraulic machines each: a Pelton turbine and a multistage pump. In recent times, the HPP was temporarily put out of service due to plant ageing damage. However, the increasing need of peak shaving capabilities by the grid (to enable a higher exploitation of renewable energy sources) made the owner evaluate its revamping as a more powerful pumped storage plant. In this regard, the owner performed a technical and economic evaluation for the HPP's recommissioning and modernization, to exploit the business opportunities given by selling energy storage services to the transmission system operator. Thus, the following decisions were taken:

- Replacement of the existing penstock with a new one;
- Replacement of both hydraulic and electrical machines with ones having the highest possible size able to fit into the existing powerhouse;

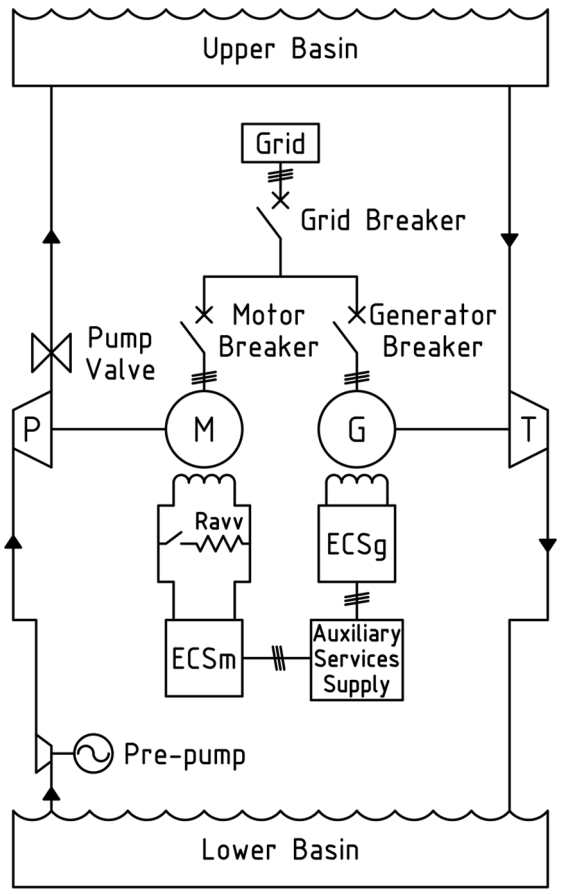

Fig. 1. Simplified scheme of the HPP in study. T – hydraulic turbine, G – generator, P – pump, M – motor, ECS – excitation control system (*m* for motor, *g* for generator).

- Separation of the generating (Pelton turbine generator) and pumping (four stage electrical driven centrifugal pump) sections;
- Overhead line refurbishment, by increasing the voltage (from 11.5 kV to 15 kV), substituting the conductors, and adding a step-up transformer to the power plant.

Regarding the electrical machines, two smooth-rotor synchronous ones were installed. One is connected to the Pelton turbine, while the other drives the pump. An additional low power pre-pump, required to overcome the difference in level between machine hall and downstream reservoir, feeds the main pump. Such an additional machine is needed, since centrifugal pumps must be filled with the fluid to be pumped in order to correctly start their operation. The new machines' data is depicted in Table 1, while the overall HPP configuration is shown in Fig. 1.

Given the electric machinery specified ratings and room arrangement, the authors have investigated the starting method among available ones, and designed a technical solution able to provide the required functions for the new HPP's pumping section, taking into account all the critical points of the system.

3. Pumping unit traditional starting methods

In the refitted HPP, the pump's synchronous motor can be connected to the generator's terminals and/or to the main grid (through a long power line), as depicted in Fig. 1.

Among the solutions listed in Table 2 [30], the mechanical one resulted unfeasible because no auxiliary hydraulic turbine or electric pony motor were available; neither the full voltage direct-on-line starting resulted feasible due to the low short circuit power at the HPP point of common coupling (due to excessive voltage drop), nor reduced voltage direct-on-line asynchronous starting as no starting reactance or reduced voltage transformer were available; also, the installation of a static converter for only providing the motor starting function was deemed not economically justifiable, thus making unfeasible a variable frequency synchronous starting.

The remaining feasible (traditional) synchronous starting methods, have been therefore evaluated to prove their effectiveness using a

Table 2
Possible starting methods for the synchronous motor pumping units [30].

Starting method	Mechanical starting		Synchronous starting			Asynchronous starting	
	Auxiliary hydraulic turbine	Auxiliary (pony) electric motor	Full frequency variation (back-to-back)	Partial frequency variation	Static converter	Full voltage direct-on-line	Reactance or transformer reduced voltage
Scheme	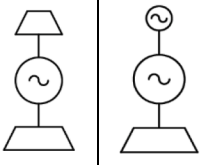						
Energy supply for start-up	Basin	Grid	Basin	Basin	Grid	Grid	Grid
Impact on electrical grid	None	Low	None	None	Low (harmonic pollution)	High	Medium-High
Need of an additional starting machine	Yes	Yes	No	No	No	No	No
Need of additional electrical equipment to be installed in the powerhouse	No	Yes	Yes	Yes	Converter can be installed in either places	No	No
Need of additional electrical equipment to be installed outside the powerhouse	No	No	No	No		No	Yes

Table 3
Differences between PFV and EPFV.

	PFV	EPFV
Motor breaker at generator startup	Open	Closed
Generator speed at which the motor starts rotating	25–50% (when motor breaker is closed)	3–4%
Motor's excitation winding	Open	Shorted through resistance

model-based design approach. In these methods, electrical motor and generator are connected in the so-called electric shaft. In such a configuration, the Pelton turbine synchronous generator provides the supply voltage to the pump synchronous motor during the startup, by operating in an electric island, so that the main grid remains unaffected (no voltage sag is provoked onto the supply grid during the motor startup, while supply voltage frequency variation at the motor terminals is made available by the generator). It is noteworthy that the presence of the Pelton turbine generator in the HPP enables the use of such starting method without requiring additional equipment.

In the traditional full back-to-back starting method [27,28], both the generator and the motor are excited when stopped, and then the turbine slowly accelerates the generator towards rated speed. In such a case the motor synchronization is achieved almost instantly, and the motor always behave like a synchronous one. Static exciters and slip rings are required for both machines, to provide the field winding's supply at zero speed. The simulations carried out according to the model-based approach shown a resulting initial loss of synchronism (as explained in Section 5). So, the back-to-back starting method resulted unsuitable.

Finally, the conventional Partial Frequency Variation (PFV) starting method [31] was evaluated. In a PFV starting, the synchronous motor starts as an asynchronous one, thanks to the torque provided by the currents flowing in the short-circuited damping windings. The power supply is delivered by the generator, whose speed is kept in the range 25–50% in order to limit the motor's slip value and thus increase its starting torque. The motor is connected to the generator only when the defined starting frequency is achieved by the generator, thus producing a startup transient due to its connection (the resulting current peak is lower than the one caused by an asynchronous starting, but still significant in respect to the one produced during a back-to-back one). Then, the motor's field winding is energized, assuring the switch towards the synchronous operation. The main issue of PFV starting method is the need of generating enough asynchronous torque to startup the motor-pump group and drive it towards an operating point where the synchronization process can happen. In this regard, simulations of the PFV shown an insufficient performance due to low starting torque. In fact, the model-based analysis pointed out the necessity of generating a higher starting torque, in order to dynamically overcome the high resistant torque of the high-power centrifugal pump. To overcome the latter issue, the novel Enhanced Partial Frequency Variation (EPFV) starting method described in Section 4 is proposed.

4. Enhanced partial frequency variation starting method

The traditional PFV method (light blue column in Table 2) requires the generator to be put in rotation at 25–50% of its rated speed without the motor connected, and then to close the motor breaker to cause the asynchronous startup of the latter (which is unexcited) [31]. Conversely, in the EPFV both the synchronous machines' breakers are closed at stand still, so that the machines start paralleled, avoiding the motor inrush transient. This also allows for the asynchronous starting of the pump to initiate at ultra-low speed (3–5% of the generator rated value), which in turn increases the torque produced by the motor due to the low slip. Moreover, the motor's excitation winding is closed on a suitably defined resistance, to further increase motor's startup asynchronous torque. The differences between traditional PFV and the EPFV are summarized in Table 3. As a result, the EPFV does not affect the upstream power grid and limits the currents magnitude like a back-to-back starting, while producing a significant torque at startup like an asynchronous one. The breakers' conditions, as well as the motor excitation winding connection during the starting process, are depicted in Table 4. The starting sequence has been designed by using a mathematical model-based design approach, which is described in Section 5. In particular, thresholds, timing, and other control parameters for the starting sequence pertaining to the electrical system have been defined through the Matlab/Simulink model shown in Fig. 2, by making several tests until a feasible combination was found. On the other hand, the hydraulic engineers fixed some of the settings for both the turbine and pump, mainly regarding their speed regulators and safety limits. The resulting starting sequence is depicted in Table 5, along with the corresponding events highlighted in the Measurement Campaign results (Section 6, Figures from 6 to 10).

Table 4
Breakers and motor excitation winding conditions.

Element \Condition	Preparation for starting	After motor synchronization	After grid connection	While pumping
Gen. Breaker	Closed	Closed	Closed	Open
Motor Breaker	Closed	Closed	Closed	Closed
Grid Breaker	Open	Open	Closed	Closed
Motor Excitation Winding	Shorted through resistance	Connected to motor ECS	Connected to motor ECS	Connected to motor ECS

5. Model based design

A mathematical model, pertaining to the Fig. 1 HPP's electromechanical part, has been developed and implemented in Matlab Simulink (Fig. 2). As mentioned above, simulations on this model allowed to define the correct starting process and set its main parameters. The mathematical model has been built upon well-known components' models, and has been previously described in [30].

The synchronous machines' model (the same is used for both) is a sixth order one, with four state variables associated to the electrical part (one field circuit and no additional circuits on the rotor *d*-axis, and a single additional circuit on the rotor *q*-axis) and two mechanical state variables [32]. Since magnetic saturations' effect on the starting sequence dynamics is negligible, these have been neglected for both the machines models. Such a model is well known, and is used for studies of electro-mechanical transients of synchronous machines [32]. Moreover, in [16] the starting of a large solid-pole synchronous motor is modeled by using such type of model, demonstrating its applicability also for machines characterized by more complex phenomena in respect to the common smooth-rotor synchronous ones used in the HPP in study. The resulting equations are included in the "Generator (1)", "Motor (2)", "Flux → Voltage", and "Voltage → Flux" blocks visible in Fig. 2. Both machines' models are expressed in *d-q* variables in their own rotating reference, and use the *per unit* notation. Therefore, in the system's mathematical model proper reference transformations have been embedded (blocks "dq Transf. 1 → 2" and "dq Transf. 2 → 1" for the dq transformation, and "p.u. change" for the *per unit* reference change). The machines' electrical connection leads to the sharing of some state variables (i.e., voltage at the terminals and stator current). Thus, the model has been arranged accordingly. For generator's mechanical part, included in the "mechanical Eq." block, the authors chose to ignore the hydraulic system's dynamic, because the Pelton turbine's response time is much higher than the one of the electrical parts. Furthermore, it is assumed that the turbine speed governor is able to properly control the

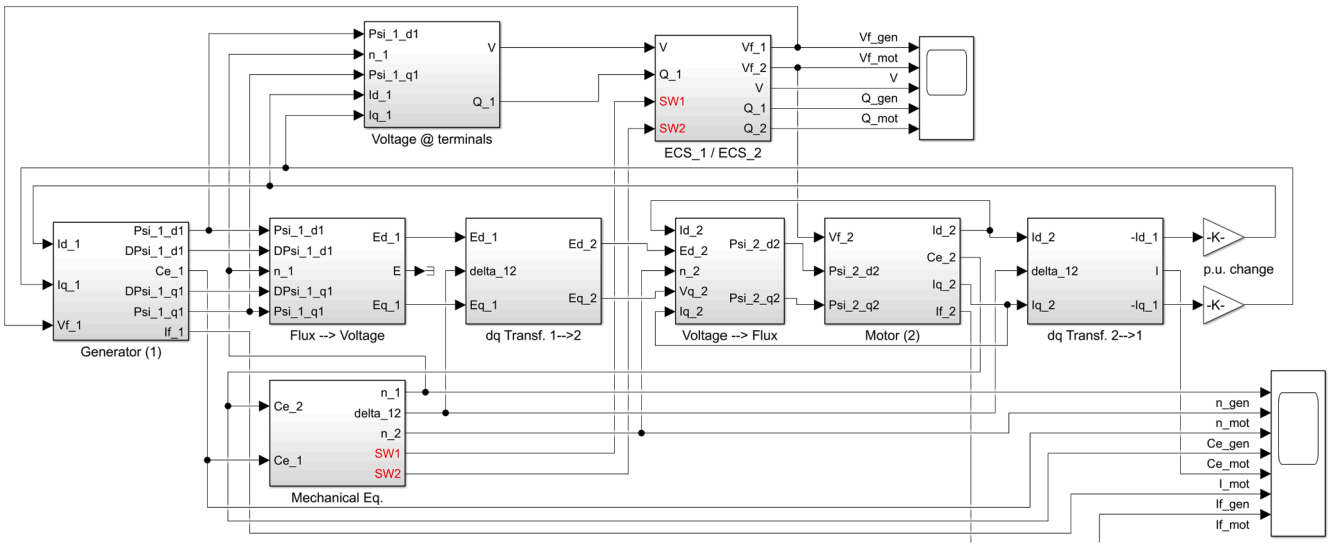

Fig. 2. Block diagram of the mathematical model for the starting sequence simulation.

Table 5
Starting sequence and corresponding events in the measurement campaign results.

Sequence steps	Event
Pump start request	0
Generator and motor breakers are closed. Grid breaker is open. All the relevant auxiliaries are supplied. The motor excitation winding is closed on a resistance (2 times the machine field resistance). The pre-pump is running, filling the main pump with water. The valve at the main pump output is closed.	Preparation for starting
The Pelton turbine is started in speed regulation, with a 25% safety speed limit (to avoid damaging the turbine-generator with an over-speed transient in case of a failed motor startup). When the turbine speed exceeds 3–5% of its rated one, the generator is excited with excitation current limited at its full load value.	1
The motor starts in asynchronous mode.	2
Once the motor reaches 2–4% of its rated speed, and 10 additional seconds have passed (to allow for the induction starting transient to settle down), the motor field winding is excited. After 4 s the resistance on the motor excitation winding is disconnected.	3
If the motor speed is still below 2% of its rated value after a given delay (i.e. 20 s), the sequence is aborted. Otherwise, the synchronization is obtained, and the generator speed is increased up to rated value. Motor follows as well in electric shaft.	4
The generator reaches rated voltage and starts following the grid reference voltage. The generator reaches rated speed and starts following the grid reference frequency. When the conditions for the correct parallel are achieved, the grid breaker is closed.	5-6-7-8
The generator is unloaded and its breaker is opened. The valve on the main pump output is opened and the water pumping operation starts.	9-10-11

hydraulic machine, by moving its speed so slowly in respect to the electromechanical transients to allow considering its variation a "quasi-static" one for the scope of this paper. For what concerns the pump, also included in the "mechanical Eq." block, it has been chosen to model its hydraulic and mechanical parts by means of a resistant torque varying with the square power of the motor speed (in centrifugal pumps power and speed have a cubic relation [33], thus making the relation between torque and speed a quadratic one). Since the water is trapped inside the pump until the startup is concluded, there is no need to include the dynamic of the rest of the pumping system's hydraulic section. Thus, the above-mentioned resistant torque emulates with sufficient accuracy the effect of the water present in the pump during the startup.

Being the starting sequence steps based on the achievement of specific inputs' thresholds, as visible in Table 5, the "mechanical Eq." block also embeds the finite state machine implementing the logic used to perform the starting sequence (logic flowchart is reported in Appendix A). The latter constitute the core of the new module that has been added to the existing ECSs control code to enable the EPFV starting function in the HPP. The "voltage @ terminals" block is then used to calculate voltage and reactive power inputs for the two regulators, based on the system state. Finally, two proportional-integral regulators are used to model the ECSs (both included in the same block called "ECS_1/ECS_2"), with proper saturations to take into account the machine capability limits. The blocks corresponding to all the model's subsections are clearly visible in Fig. 2.

Simulation results in are shown in Fig. 3, where the excitation variables (I_{ecc}, V_{ecc}), machines speeds (*speed*), and terminal voltages (magnitude of the Park vector, $|V|$) are depicted in physical units. The feasibility of the partial frequency variation synchronous starting method for the HPP in study has been tested by means of subsequent simulations, where all of its relevant parameters (time and speed thresholds, order of the steps, etc.) have been varied until the results of the simulated startup transient met the required performance. Besides demonstrating the sequence feasibility, the simulations provided useful info to correctly set the starting sequence steps and its parameters, thus applying a model/based design approach for the exploitation of the starting method in the HPP. As can be seen from Table 5, the EPFV is based on specific time and speed thresholds, along with the HPP breakers' operations. By testing several different parameters, it has been possible to find the correct combination of time/speed thresholds and sequence steps capable of enabling the pump startup.

It is worth noticing that the back-to-back traditional starting method, which was the first option investigated for the case study, has been tested by means of the above-described simulator, and subsequently discarded. This because the simulations highlighted a loss of synchronism during the startup due to the high inertia of the motor-pump group and the resistant torque of the water in the pump.

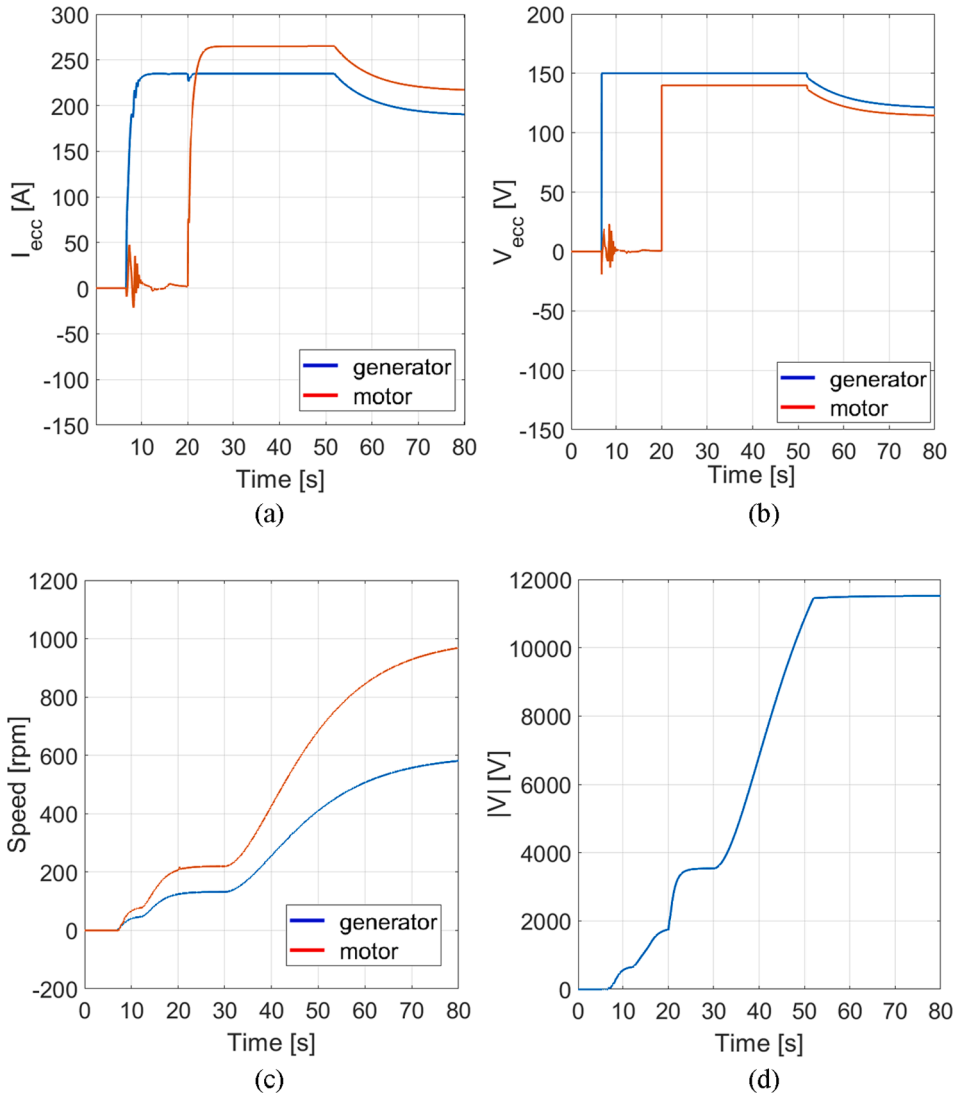

Fig. 3. Simulated generator and motor excitation variables: a) excitation current, b) excitation voltage, c) rotor speed, and d) voltage at terminals.

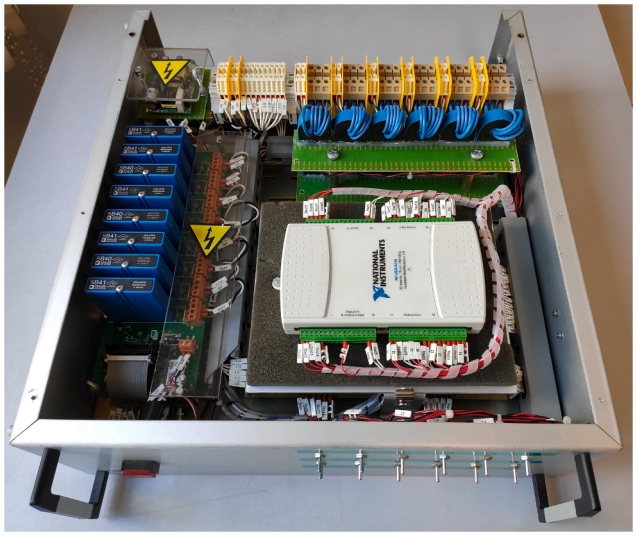

Fig. 4. Measurement system installed during the commissioning of the starting sequence.

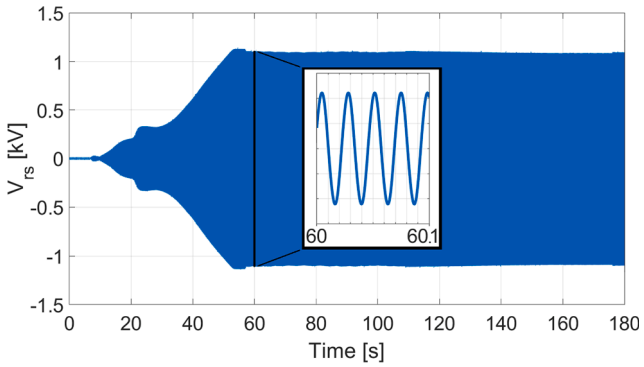

Fig. 5. Example of a measured sinusoidal variable (line-to-line voltage).

6. Implementation and experimental tests

6.1. Digital excitation control system platform

Authors' experiences in developing real-time control devices (hardware and software platforms) have been already documented in the field of primary [29] and secondary [34] voltage regulation. In this regard, the use of industrial or embedded PCs with real-time operating system gives great flexibility to the solution. In fact, a digital ECS is a PC with a General-Purpose Processor (GPPs), patched with the Linux Real Time Application Interface (RTAI), and suitable analog and digital input/output interfaces [35]. Thanks to the onboard software, such ECS combines conventional voltage control functions with a finite state machine, which provides all logic and safety standard functions. Such an open software architecture also allows implementing new functions by means of additional software modules, which can be implemented after the field installation or even after years of operation. Thus, the hardware and software architecture of a digital ECS ensures an increased system's flexibility. A mathematical model of the power plant is also coded in the digital ECS, providing an onboard simulator for Hardware-In-the-Loop tests and commissioning. The tests can be done either in factory or at the plant, by diverting the ECS input–output signals to the simulator through proper software flags. Such an operation is in fact a step towards the so-called Digital Twin concept [36,37] in the field of power systems' control, and it is enabled by the abundant computational power of modern GPPs.

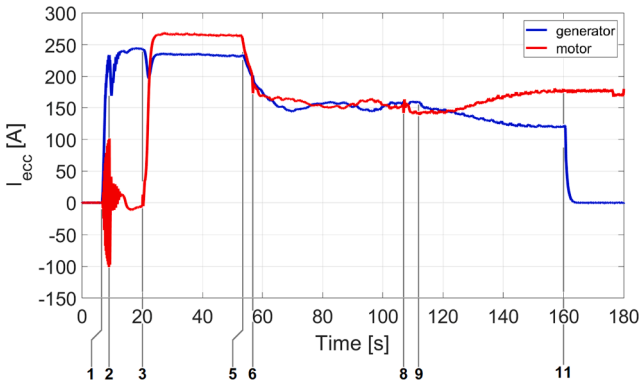

Fig. 6. Generator and motor excitation current, measured during the startup process.

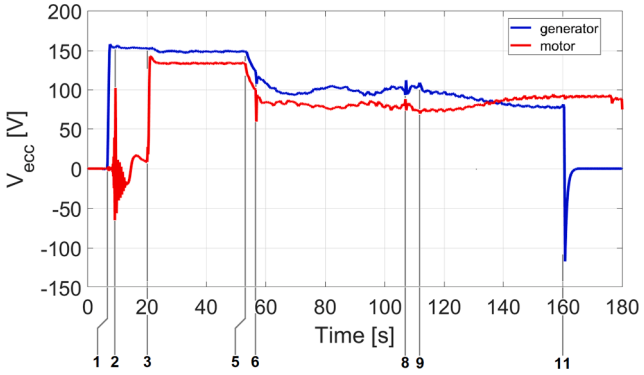

Fig. 7. Generator and motor excitation voltage, measured during the startup process.

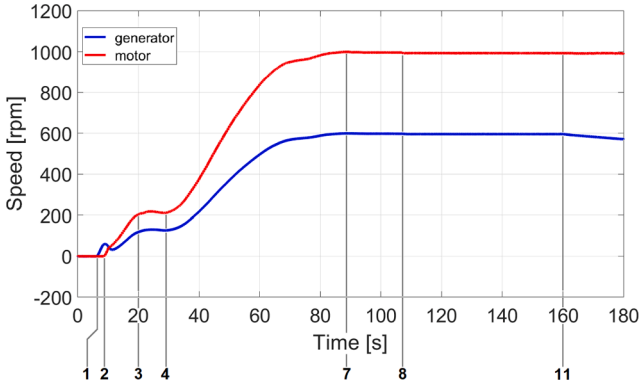

Fig. 8. Generator and motor speed, measured during the startup process.

For the application presented in this paper, the use of a COTS hardware, coupled with an open software platform, allowed to implement the starting sequence directly into the ECSs, through a new software module integrated in each ECS. In fact, the two machines were already equipped with ECSs for performing conventional primary voltage regulation, leading to the possibility to exploit their flexibility to implement the coordinated starting function without relying on additional hardware (and related costs).

6.2. Implementation of the starting sequence in the ECSs

After having validated the EPFV in simulations, the overall starting sequence has been applied to the HPP. The starting sequence has been

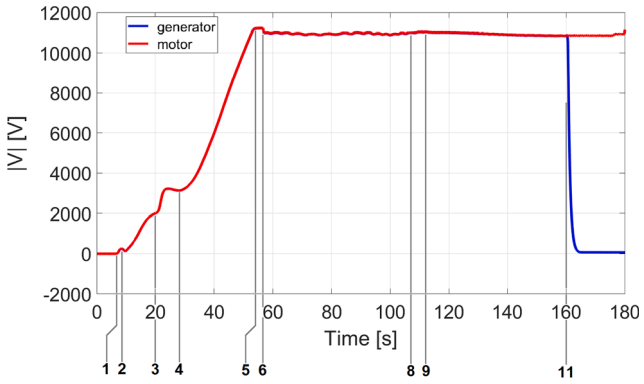

Fig. 9. Generator and motor Park voltage module at machines' terminals, measured during the startup process.

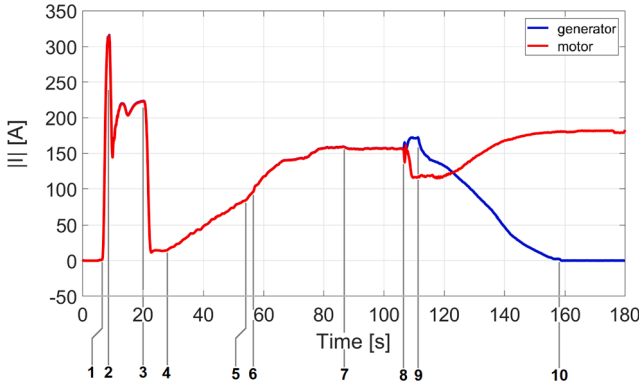

Fig. 10. Generator and motor Park current module at machines' terminals, measured during the startup process.

coded in both the generator's (Pelton turbine) and motor's (pump) ECSs, by means of proper software modules. During the starting sequence the two ECSs take over system control, feeding the HPP automation system with the required set of signals to perform the motor startup. In addition to that, the two ECSs work autonomously by taking as input the variables coming from field measurement units (i.e. breaker states and machines speeds) of both electrical machines. Then, each ECS elaborates independently the proper input/output control signals, without the need of any communication channel with the other ECS. This is enabled by the careful definition of time/speed thresholds made through the mathematical model exploitation (model-based design approach), which makes it possible for each ECS to independently perform its control action on the basis of its own input/output signals, as well as to detect the failure of the overall sequence and abort the operation if needed. To this aim, the steps advancement and the operation failure detection are obtained by checking the value of specific inputs, and by comparing them to the set thresholds and to the internal clock, as shown in the flowchart in Appendix A. If a set of variables reach the set thresholds before the time limit runs out, the next set of actions defined by the sequence is applied. Otherwise, if a variable takes too much to reach the required threshold, the sequence is considered as failed and thus aborted. The result is a coordinated control of the system (during the startup operation) obtained without a centralized coordinator agent, by only using distributed control systems (Appendix A). As a result, the starting sequence is fully automated, which is an advantage since the hydroelectric power plant is unmanned, and it is only monitored remotely. Moreover, the sequence can be applied with a reduced impact on the HPP, since no additional equipment is required, and allows the correct pump start, its grid synchronization, and the subsequent turbine stop with no disturbance to the power grid.

6.3. Measurement setup

During the system commissioning, a dedicated measurement system has been installed. The measurement activity had the goals of verifying the correct system operation, providing data for solving possible issues, and validating the previously performed simulations. The measurement system (shown in Fig. 4) is composed by a set of signal adapters and an isolated USB multifunction I/O device (32 Analog Inputs @ 16-Bit, 250 kS/s; 2 Analog Outputs @ 250 kS/s, 8 Digital Inputs, 8 Digital Input/Outputs). Such an instrument makes it possible to interface the current and voltage transformers already installed in the power plant with a data collecting PC. The signals have been acquired with a 3 kHz sampling frequency for each channel.

6.4. Measurement campaign results

The data measured during a complete startup sequence is shown in Figures from 5 to 10. Specifically, in Figs. 6 and 7 the excitation currents and voltages for the two machines are depicted (taken at the excitation windings' terminals). Conversely, Fig. 8 shows the speed of the two machines, while Figs. 9 and 10 depict the Park vectors magnitude of voltage and current, respectively. Regarding the latter, the measurement system acquires two line-to-line voltages (e.g., Fig. 5) and two phase currents only, which are sufficient for the scope being the system a three-wire one. The Park vectors are then calculated off-line by using the information coming from the measured variables (voltage, current, and speed). Finally, high frequency noise has been removed from the data using a moving-average digital filter. In particular, this filter has been chosen in place of a standard low-pass one to avoid introducing a phase change into the variables used for calculating the Park vectors. The need of evaluating a filter window that extends both before and after the considered data point is not an issue, the data being processed offline.

Figures from 6 to 10 refer to the following time events, highlighted with a number:

1. Pump start request ($t = 0$), and preparation for starting ($0 < t < 6.5$ s). The generator and the motor breakers are closed, while the grid breaker is open. The motor winding is closed on a resistance, to avoid short-circuiting the exciter and to increase the torque during the asynchronous starting. The pump output valve is closed and the pre-pump is running, filling the main pump with water.
2. The Pelton turbine is activated. A safety limit on its speed governor is set, at 25% of the rated speed, to avoid over-speeding if the motor startup fails. When the generator speed rises above 3–5% of the rated one, its ECS is activated. From this moment onwards, the ECS is in automatic voltage control, with excitation current limited to the full-load one. Due to the reduced speed, the magnitude of the voltage at machine's terminals is reduced (Fig. 9).
3. The motor starts rotating in response to the asynchronous torque. The induced currents and voltages in the excitation circuit are clearly visible in Figs. 6 and 8. The typical behavior of asynchronous rotor currents is evident (i.e. frequency varying currents, from supply frequency to nearly steady state). The braking torque caused by the motor's starting current peak (Fig. 10) leads to a temporary dip in the generator's speed and in its excitation current. Once the motor speed rises above 2–4% (at circa 10 s), the motor ECS waits additional 10 s for the induction starting transient to settle down.
4. After the 10 s delay, the voltage control loop of the motor ECS is activated, with excitation current limited to the full load one. The resistance is still connected to the motor excitation winding. This is the start of the synchronization process with the generator. Given the low speed, the rated voltage cannot be achieved in the system. Thus, the two ECSs saturate at the maximum allowed

excitation current (i.e. the full load one), as can be clearly seen in Fig. 6. After 4 s from the motor's excitation voltage control activation, the resistance on the excitation winding is disconnected.
5. Generator and motor are synchronized. The Pelton turbine speed governor can now progressively accelerate towards rated speed, and the motor accelerates accordingly. The voltage at machines' terminals rises, as expected.
6. Rated voltage is achieved (as can be seen in Fig. 9). The two ECSs start regulating the excitation currents.
7. Grid voltage is now assumed as reference set point for the ECSs, to prepare for the synchronization with the grid. Due to that, the Fig. 9 voltage has a small drop, from the rated value to the grid one.
8. Both generator and motor have reached the rated speed. The grid frequency is applied as reference for the turbine speed governor, to enable grid synchronization.
9. The system is ready to be synchronized with the grid, thus the grid breaker is closed. The paralleling transient that happens afterwards is clearly visible in the machines' currents (shown in Fig. 10). The motor is now correctly started and supplied by the grid, ready to start the water pumping process. The latter is achieved by means of the opening of the hydraulic valve installed on the pump output, which happens from 120 s onwards.
10. The procedure for disconnecting the generator is started. Its ECS controls the de-excitation until the reactive power at the machine terminals becomes zero, while the turbine speed governor starts closing the hydraulic valve to reduce the active power produced.
11. Generator's active and reactive power are now zero (losses apart). Thus, its breaker is opened.
12. The generator is de-excited. The ECS rapid de-excitation function provokes a negative excitation voltage (the negative spike in Fig. 7) to nullify the excitation current (as shown in Fig. 6). The Pelton natural stopping process starts, as can be seen from the speeds slight decrease inception in Fig. 8.

The results of the measurement campaign, showing a full startup sequence of the 5 MVA pump in the real HPP, demonstrate the effectiveness of the proposed solution. Indeed, the EPFV allows the motor asynchronous starting at ultra-low speed despite the high torque required to start moving the centrifugal pump, at the same time limiting the transients magnitude for the machines. The latter is particularly evident considering the Park current at machines terminals (Fig. 10), whose maximum magnitude is only 35% higher than the rated current for the motor. Moreover, it is demonstrated that the proposed starting system is capable of enabling the pumping function without affecting the upstream power grid and without the need of additional equipment.

6.5. Mathematical model validation

The comparison of numerical and experimental results shows a practical full matching of all the time domain variable transients. The only small appreciable differences among them are related to side effect phenomena which do not affect the model-based design, and which can be explained as follows:

- The excitation current I_{ecc} is different between the simulation and the measurements from 55 s onwards, due to the start of the grid voltage reference tracking at point 6 in the real system (such event has not been included in the mathematical model);
- The same difference can be appreciated for the excitation voltages V_{ecc} from 55 s onwards, for the same reason depicted for I_{ecc}. Moreover, the simplification hypotheses applied in the mathematical model reduce its capability of correctly simulating high frequency transients, thus leading to the visible difference between simulation and measurement results visible in the first 10 s (when the motor's rotor is still, or just started rotating, and thus is subject to the variable magnetic field originated by the stator);
- Regarding the speed, the same effect depicted for V_{ecc} is appreciable in the first 10 s, where the generator lacks the first speed drop;
- The only difference regarding the Park voltage module at machines' terminals among simulations and measurements is the lack of the voltage drop caused by the grid tracking action in the simulation results (which happen at point 6 in the real system).

7. Conclusions

The pumped storage is one of the most viable energy storage systems for making possible a sustainable and massive penetration of renewables in the electrical power system. A novel starting sequence for a pumped-storage HPP has been proposed, named EPFV, based on a mathematical model-based design approach valid for the electromechanical transients' domain. EPFV starting sequence improves conventional PFV one, by coupling the advantages of back-to-back starting (limited currents during startup) with the ones of asynchronous starting (high starting torque), with no impact on the power grid during its execution. Using modern digital excitation control system, the EPFV starting of a large pump synchronous motor has been realized by means of proper software modules and the routing of HPP measurement and breaker signals. The EPFV starting sequence has been implemented in a revamped HPP, demonstrating its capability in ensuring the correct starting of the pump without affecting the power grid, and without requiring further additional electrical or starting equipment.

The results of the simulations, as well as the results from the commissioning tests on the real system, demonstrate the feasibility of the proposed starting solution and its effectiveness in terms of electromechanical transient performance.

CRediT authorship contribution statement

Andrea Vicenzutti: Validation, Data curation, Writing - original draft, Writing - review & editing, Visualization. **Massimiliano Chiandone:** Software, Validation, Data curation. **Vittorio Arcidiacono:** Conceptualization, Methodology, Formal analysis, Investigation, Supervision. **Giorgio Sulligoi:** Investigation, Writing - original draft, Writing - review & editing, Supervision.

Declaration of Competing Interest

The authors declare that they have no known competing financial interests or personal relationships that could have appeared to influence the work reported in this paper.

Appendix A

The logic flowchart depicting the logic used to perform the starting sequence proposed in this paper (i.e., the EPFV method) is here depicted (Fig. A1). Each rectangular box identified by a letter is a step of the logic sequence, while the bold arrows depict the direction of logic steps change. The items on the right of the steps, indicated by the dotted arrow and enclosed in a rounded edges box, are the actions that need to be performed in that specific step. The set of items represented on the left of the steps, which are connected to them by dashed lines, are the logic checks that need to be verified in order to proceed with the next step of

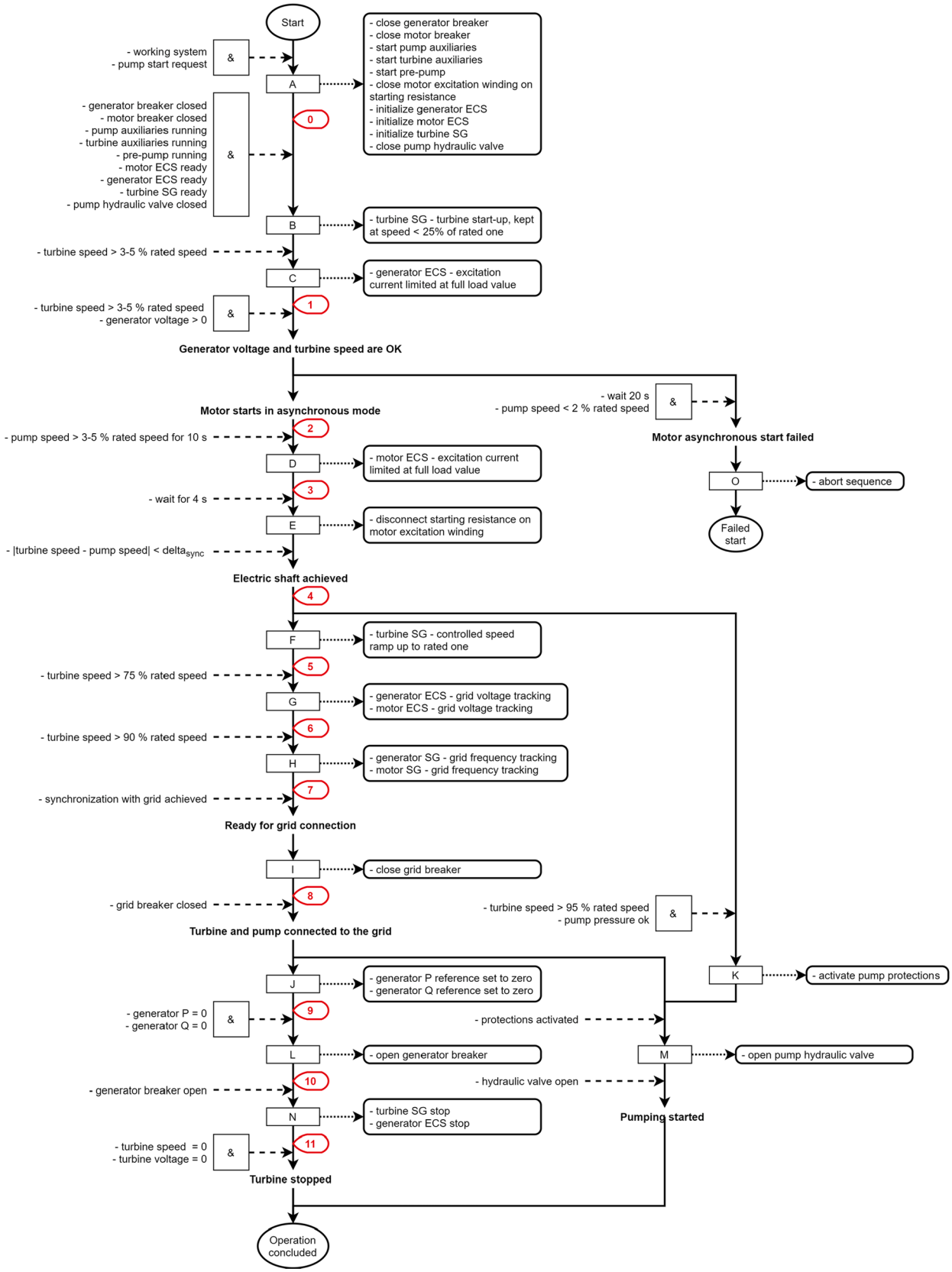

Fig. A1. Logic flowchart depicting the logic used to perform the EPFV starting sequence.

the logic sequence. Finally, the red labels show the correlation between the starting sequence logic steps and the highlighted events in the measurement results.

References

[1] Chen H, Cong TN, Yang W, Tan C, Li Y, Ding Y. Progress in electrical energy storage system: A critical review. Prog Nat Sci Jan 2009;19(3):291–312.
[2] Denholm P, Ela E, Kirby B, Milligan M. The role of energy storage with renewable electricity generation. National Renewable Energy Laboratory, CO (USA), Jan. 2010 [Online]. Available: http://www.nrel.gov/docs/fy10osti/47187.pdf.
[3] Whittingham MS. History, evolution, and future status of energy storage. In: Proceedings of the IEEE, vol. 100, no. Special Centennial Issue, pp. 1518-1534, 13 May 2012.
[4] Ibrahim H, Ilinca A, Perron J. Energy storage systems—Characteristics and comparisons. Renew Sustain Energy Rev 2008;12(5):1221–50.
[5] Malik AS, Cory BJ. Assessment of pumped storage plant benefits in fuel budgeting and operational planning. In: 1991 International Conference on Advances in Power System Control, Operation and Management, APSCOM-91., Hong Kong, vol.1; 1991, pp. 379–384.
[6] Chun-Tian Cheng, Xiong Cheng, Jian-Jian Shen, Xin-Yu Wu. Short-term peak shaving operation for multiple power grids with pumped storage power plants. Int J Electr Power Energy Syst May 2015; 67: pp. 570–581.
[7] Raul NS, Necsulescu C. Economics of energy storage devices in interconnected systems - A new approach. IEEE Trans Power Apparatus Syst 1984; PAS-103(6): pp. 1217–1223.
[8] Li H, Tan H, Hu S. Study on dynamic benefits and external economy of pumped-storage plant. In: 2006 International Conference on Power System Technology, Chongqing; 2006, pp. 1–8.
[9] Kloess M, Zach K. Bulk electricity storage technologies for load-leveling operation – An economic assessment for the Austrian and German power market. Int J Electr Power Energy Syst 2014; 59: pp. 111–122.
[10] Kanakasabapathy P. Economic impact of pumped storage power plant on social welfare of electricity market. Int J Electr Power Energy Syst 2013;45(1):187–93.
[11] Terna S.p.A. Piano di Sviluppo 2020 [Online]. Available: https://download.terna.it/terna/Piano%20di%20Sviluppo%202020_8d7db1ffa4ca9e7.pdf.
[12] Pickard WF. The history, present state, and future prospects of underground pumped hydro for massive energy storage. Proc IEEE 2012; 100(2): pp. 473–483.
[13] El-Mahayni R, Al-Qahtani K, Al-Gheeth AH. Large synchronous motor failure investigation: measurements, analysis, and lessons learned. IEEE Trans Ind Appl 2016; 52(6): pp. 5318–5326.
[14] Qi Y, Geng H, Du T, Li Y, Yin X, Xu H. Influence of variable frequency starting parameters on synchronous motor starting. In: 2019 IEEE International Conference on Mechatronics and Automation (ICMA), Tianjin, China; 2019. pp. 336–341.
[15] Castagnini A, Känsäkangas T, Kolehmainen J, Termini PS. Analysis of the starting transient of a synchronous reluctance motor for direct-on-line applications. In: 2015 IEEE International Electric Machines & Drives Conference (IEMDC), Coeur d'Alene, ID; 2015, pp. 121-126.
[16] Mi CC, Li Y, Karmaker H. Modeling of the starting performance of large solid-pole synchronous motors using equivalent circuit approach. IEEE Trans Magn Dec. 2009;45(12):5399–404.
[17] Canay M. Methods of starting synchronous machines. Brown Boveri Rev 1967; 54 (9): pp. 630–637.
[18] Nevelsteen J, Aragon H. Starting of large motors-methods and economics. IEEE Trans Ind Appl 1989; 25(6): pp. 1012–1018.
[19] Concordia C, Crary SB, Kilbourne CE, Weygandt CN. Synchronous starting of generator and motor. Trans Am Inst Electr Eng 1945;64(9):629–34.
[20] Concordia C, Brown PG, Miller WJ, Wuosmaa L. Synchronous starting of motor from generator of small capacity. In: IEEE Transactions on Power Apparatus and Systems, vol. PAS-86, no. 10, pp. 1215-1226, Oct. 1967.
[21] Das JC, Casey J. Characteristics and analysis of starting of large synchronous motors. In: 1999 IEEE Industrial and Commercial Power Systems Technical Conference (Cat. No.99CH36371), Sparks, NV, USA; 1999.
[22] Karmaker H, Mi Chunting. Improving the starting performance of large salient-pole synchronous machines. IEEE Trans Magn 2004; 40(4), pp. 1920–1928.
[23] Li Xiaolu, Kou J, Han Xiao, Gao Q, Li Gang, Xu D. Research on soft starting control strategy for LCI-fed synchronous motor. In: 2016 IEEE 8th International Power Electronics and Motion Control Conference (IPEMC-ECCE Asia), Hefei; 2016: pp. 1858-1862.
[24] Pérez-Loya JJ, Abrahamsson CJD, Evestedt F, Lundin U. Demonstration of synchronous motor start by rotor polarity inversion. IEEE Trans Ind Electron 2018; 65(10):8271–3.
[25] Duong QH, Nguyen HC, Nguyen HQ, Nguyen C. Application of fuzzy control algorithm to start a large - capacity synchronous motor. In: 2020 5th International Conference on Green Technology and Sustainable Development (GTSD), Ho Chi Minh City, Vietnam; 2020, pp. 574–581.
[26] LeDoux K, Visser PW, Hulin JD, Nguyen H. Starting large synchronous motors in weak power systems. IEEE Trans Ind Appl 2015.;51(3):2676–82.
[27] Konidaris DN. Investigation of back-to-back starting of pumped storage hydraulic generating units. IEEE Trans Energy Convers 2002;17(2):273–8.
[28] Osburn GD, Atwater PL. Design and testing of a back-to-back starting system for pumped storage hydrogenerators at Mt. Elbert Powerplant. IEEE Trans Energy Convers 1992;7(2):280–8.
[29] Sulligoi G, Chiandone M, Arcidiacono V. A real-time device for smart excitation control systems. In: Proc. of AEIT National Conference, Milano (Italy); 2011, pp. 1–5.
[30] Chiandone M, Arcidiacono V, Sulligoi G. Electric shaft starting sequence for synchronous generator in hydroelectric pumped storage station using smart exciter. In: 2018 IEEE Power & Energy Society General Meeting (PESGM), Portland, OR; 2018, pp. 1–5.
[31] Hammons TJ, Loughran J. Starting methods for generator/motor units employed in pumped-storage stations. In: Proceedings of the Institution of Electrical Engineers, vol. 117, no. 9, pp. 1829–1840, September 1970.
[32] Marconato R. Synchronous Machines. In: Electric Power Systems, 2nd Edition, ed. CEI – Italian Electrotechnical Committee; 2002.
[33] Gevorkov L, Rassõlkin A, Kallaste A, Vaimann T. Simulation study of a centrifugal pumping plant's power consumption at throttling and speed control. In: 2017 IEEE 58th International Scientific Conference on Power and Electrical Engineering of Riga Technical University (RTUCON), Riga; 2017, pp. 1-5.
[34] Sulligoi G, Chiandone M, Arcidiacono V. NewSART automatic voltage and reactive power regulator for secondary voltage regulation: Design and application. In: 2011 IEEE Power and Energy Society General Meeting, Detroit, MI, USA; 2011, pp. 1–7.
[35] Chiandone M, Cleva S, Sulligoi G. PC-based feedback acceleration control using Linux RTAI. In: 2009 13th European Conference on Power Electronics and Applications, Barcelona; 2009, pp. 1–8.
[36] Liu Mengnan, Fang Shuiliang, Dong Huiyue, Xu Cunzhi. Review of digital twin about concepts, technologies, and industrial applications. J. Manuf. Syst. 2021;58 (Part B):346–61.
[37] Schluse M, Priggemeyer M, Atorf L, Rossmann J. Experimentable digital twins—streamlining simulation-based systems engineering for industry 4.0. IEEE Trans Ind Inf April 2018;14(4):1722–31.